

SETTLEMENT MITIGATION OF CYLINDRICAL TANKS FOUNDED ON WEAK SOIL UNDER STATIC LOADING

Sief El-Islam M. Abbas^{1*}, Ibrahim A. El Arabi², M. M. El Gendy³

¹ Demonstrator, Department of Civil Engineering, Faculty of Engineering, Sinai University, Al-Arish, Egypt, email: sief.elislam@su.edu.eg

² Assoc. Professor, Head of Civil Dept, Delta Uni. for Science and Technology, Egypt, email: Ibrahim.alarabi@deltouniv.edu.eg.com

³ Professor of Geotechnical and Foundation Engineering, Faculty of Engineering, Port Said University, Egypt email: melgendy@elpla.com

*Corresponding author, DOI: 10.21608/PSERJ.2024.249595.1284

ABSTRACT

The issue of soft soil settlement has been a significant concern for several decades, prompting researchers to explore various approaches to enhance soft soil conditions and mitigate excessive soil settlement. Commonly employed techniques in this field include stone columns, encased stone columns, and foundation level adjustment. In the present study, a parametric investigation was conducted to assess the effectiveness of these different techniques in reducing expected excessive settlement for reinforced concrete cylindrical tanks founded on Port-Said weak soil. A 3D finite element model was developed using PLAXIS 2D/3D to simulate a completely symmetric cylindrical tank. The numerical model replicates the typical construction and operation stages of the tank, employing Mohr-Coulomb and Hardening constitutive models to represent the layered soil in the analysis. The findings of this study aim to provide valuable design recommendations for constructing circular wide storage tanks in the Port-Said district, addressing the specific challenges posed by soft soil settlement.

Keywords: cylindrical tanks, stone columns, encased stone columns, consolidation, PLAXIS 3D

Received 18-11-2023,

Revised 14-12-2023,

Accepted 8-1-2024

© 2023 by Author(s) and PSERJ.

This is an open access article licensed under the terms of the Creative Commons Attribution International License (CC BY 4.0).

<http://creativecommons.org/licenses/by/4.0/>



1 INTRODUCTION

For several decades, construction on soft soil has presented a significant challenge within the geotechnical engineering community due to excessive settlement. The need to address excessive soil settlement becomes increasingly critical with the continuous growth of infrastructure development. So, researchers have been drawn to explore various approaches aimed at enhancing soft soil conditions and mitigating settlement-related challenges. Commonly employed techniques are stone columns, encased stone columns, and foundation level adjustment. Stone columns act as reinforcing material, increasing the overall strength and stiffness of the compressible soft soil, accelerating the consolidation as it provides a shortened drainage path, and hence reducing the resulting settlement. This literature review explores some recent advancements in addressing soft soil settlement, focusing on a parametric investigation conducted to assess the effectiveness of these techniques

in the context of reinforced concrete cylindrical tanks founded on Port-Said weak soil.

Considerable research has been conducted to investigate excessive settlement in soft soil. Wang [1] presented an analytical solution for the consolidation of soft soil foundations reinforced by stone columns under time-dependent loadings. Deb and Das [2] examined the stress distribution on the ground reinforced by stone columns under a cylindrical storage tank. They modeled the soft soil, stone columns, and granular fill using mechanical elements, with the floor slab treated as a flexible thin plate. Das and Deb [3] explored the response of a cylindrical storage tank foundation on stone column-reinforced ground. Zukri and Nazir [4] reviewed methodological approaches for 2D and 3D numerical models of stone columns, discussing appropriate numerical techniques and constitutive models. Muzammil et al. [5] investigated the behavior of geosynthetic encased stone columns under a circular oil

storage tank, comparing it with ordinary stone columns under the same in situ conditions using PLAXIS 3D. El-Gendy [6] numerically analyzed the behavior of circular tanks resting on multi-layer soil under both static and cyclic loading using ELPLA software.

The research under consideration adopts a comprehensive approach, utilizing a 3D finite element model developed using PLAXIS 2D/3D. The study specifically targets the unique challenges posed by soft soil settlement in the Port-Said district, offering insights that could have broad implications for circular wide storage tank construction in similar geotechnical contexts. The numerical model replicates the various construction and operation stages of a completely symmetric cylindrical tank. To capture the complex behavior of the layered soil, the analysis employs Mohr-Coulomb and Hardening constitutive models.

The primary objective of this parametric investigation is to provide valuable design recommendations for mitigating excessive settlement in reinforced concrete cylindrical tanks. By examining the effectiveness of stone columns, encased stone columns, and foundation level adjustment, the study aims to contribute practical insights into the selection and implementation of suitable ground improvement techniques for circular wide storage tanks in soft soil conditions. The findings of this research hold particular relevance for construction projects in the Port-Said district, offering a tailored understanding of the challenges associated with soft soil settlement.

2 DESCRIPTION OF THE NUMERICAL MODEL

Many researchers have adopted numerical simulation to analyze a variety of geotechnical problems, including stone columns as well as encased stone columns because the experimental procedures were prohibitively expensive [4, 5, 7]. Numerical experiments for cylindrical tanks resting on layered soil were performed herein with the PLAXIS 2D/3D. For creating the finite element model using PLAXIS, one has to define the problem geometry, material properties, boundary conditions, and loads.

2.1 Geometry of the finite element model

Consider the 13.0 [m] diameter by 3.5 [m] height circular tank shown in Figure 2.1. Both the tank base and wall have a constant thickness of 0.2 [m]. The soil depth of the finite element model was taken at 60 [m], the same as the borehole depth, while the circular soil mass's radius was equal to 32.5 [m], five multiples of the tank radius, to provide an acceptable analysis accuracy.

The tank was assumed to be underlain by a typical layered Port Said soil, which is characterized by a 30-35 [m] thick deposit of soft clays/silts with sand interlayers resting on a compacted clay layer.

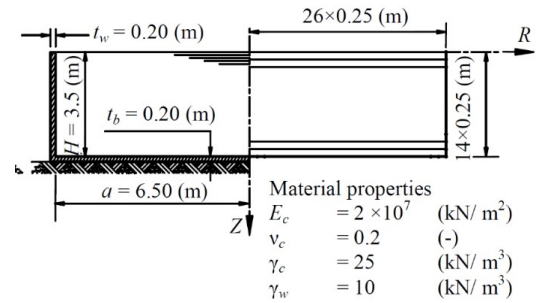


Figure 2.1: Geometry and F.E. mesh of a circular tank, El-Gendy [6].

2.2 Material modeling

The reinforced concrete base and wall of the tank were considered as isotropic elastic material with the parameters given in Figure 2.1 (the unit weight of concrete was taken as 25 [kN/m³], Young's modulus equals 2×10^7 [kN/m²], and Poisson's ratio equals 0.2).

The tank is assumed to be underlain by a typical layered Port Said soil profile, as shown in Figure 2.2, whose geotechnical properties have been given by [8, 9]. It's a common practice to replace approximately two meters of the surface soil with a gravel/sand mix stiff soil [6]. The compressibility modulus of the replacement layer is 100,000 [kN/m²] with a saturated unit weight of 20.81 [kN/m³]. Therefore, the subsoil stratification is classified into six main layers as follows:

- [0.00 to 2.00 m]: Gravel, Sand,
- [2.00 to 7.00 m]: Silty clay, very soft,
- [7.00 to 12.00 m]: Sand, fine, loose to dense,
- [12.00 to 33.00 m]: Clay, soft to firm,
- [36.00 to 36.00 m]: Sand, medium to very dense, and
- [36.00 to 60.00 m]: Clay, very stiff to hard.

The first, third, and fifth layers were modeled using the Mohr-Coulomb soil model with drained drainage, where the stiffness and strength are defined in terms of effective properties. The groundwater permeability coefficient was taken as 0.0202×10^{-3} [m/day]. The angle of internal friction was assumed to be 30°, and the cohesion was considered zero. The mechanical properties of each layer are provided in Figure 2.2.

The Hardening soil model with undrained (B) drainage type was selected for the second, fourth, and sixth layers. In this model, stiffness is defined in terms of effective properties, and strength is represented by undrained shear strength, set at 20 [kN/m²] based on Banupriya et al. (2015) [10]. The mechanical properties of each layer are detailed in Figure 2.2.

The Over-Consolidation Ratio (OCR) for layer two was calculated from the experimentally obtained undrained shear strength [6], resulting in an OCR of approximately 1.6-1.2 adopted for layer 2. Layer 4 was assumed to be normally consolidated. For layer 6, laboratory tests indicated a pre-consolidation pressure exceeding 450 [kN/m²], suggesting that the vertical

stress increase does not fall within the normally consolidated range.

The initial void ratio (e_0) of the soft layers is determined as a function of the compression index (C_c), according to Nishida (1956) [11]. It can be expressed as follows:

$$C_c = 0.54(e_0 - 0.35) \quad 2-1$$

The void ratio e_0 was taken as 1.55, 1.10, and 0.72 for layers 2, 4, and 6, respectively. On the other hand, the coefficient of permeability (k_v) for soft layers can be obtained from the coefficient of volume change ($m_v=I/E_s$) according to Terzaghi et al. (1996) [12] through the relation:

$$C_v = \frac{k_v}{\gamma_w m_v} \quad 2-2$$

Where γ_w is the unit weight of the water, and m_v is the coefficient of volume change ($m_v=I/E_s$). k_v was taken as 0.0074, 0.0013, and 0.0010 [m/ year] for layers 2, 4, and 6, respectively.

2.3 Meshing

This problem has been investigated numerically by El-Gendy [6] using a multi-layer soil model and an axis-symmetric finite element analysis by ELPLA software [8], as the cylindrical tank and soil mass are concentric. The right-hand side half of the sectional elevation of the tank depicted in Figure 2.1 shows the mesh discretization of the axis-symmetric finite element model adopted by El-Gendy [6], where the 13.0 [m] diameter circular base was divided into 26 ring elements, each of 0.25 [m] uniform width. The tank wall was divided into 14 cylindrical elements, each of 0.25 [m] constant height.

In the present simulation using PLAXIS 2D/3D, only a quarter of the full soil mass and the cylindrical tank were modeled. Then, symmetry conditions were applied to simulate the rest of the structure. The tank base and walls were modeled by the 2D 6-node triangular shell element available in the element library of PLAXIS, whereas the 10-node tetrahedral element was used to model the soil mass. One has to ensure that the mesh is fine enough to capture the important details but not overly dense to avoid excessive computation time. A medium element disruption generates a mesh with a maximum element dimension of 4.837 [m] for soil volumes and 1.0 [m] for tank elements, and the software uniformly distributes the mesh size in between. The model contains 58782 soil elements for 39139 nodes with an average element size of 2.825 [m]. The generation of negative interface elements under the tank base plate was essential to allow for proper modelling of soil-structure interaction [9, 13].

2.4 Loads and boundary conditions.

The Base plate of the tank was subjected to a surface uniform distributed load of $\sigma_z = -34.34$ [kN/m²] to simulate vertical water pressure, and the wall plate was subjected to a Perpendicular vertical increment surface load of $\sigma_{n,inc} = 9.81$ [kN/m²/m], and $Z_{ref} = 3.5$ [m] to simulate horizontal water pressure.

To simulate only a single quarter of the model, the deformation condition was set as normally fixed for all

directions except Z-Min, which was set as fully fixed, and Z-Max, which was set as free. Additionally, the groundwater flow was assumed to be closed at the bottom of the model due to its impermeable soil and tangentially at X-Min and Y-Min due to symmetry.

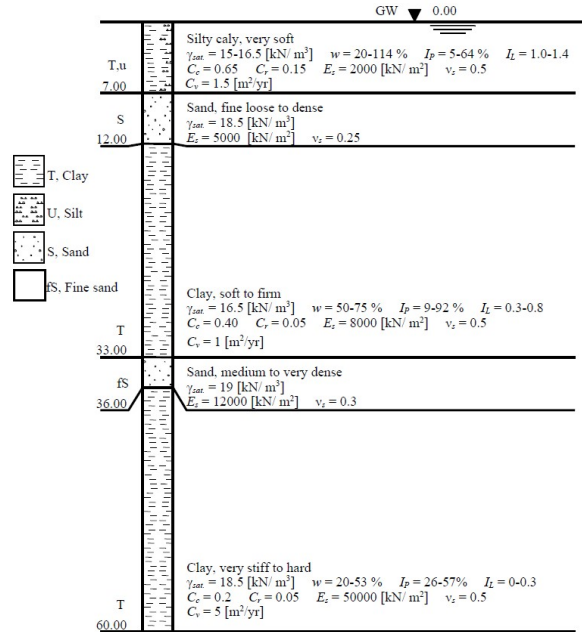


Figure 2.2: Typical soil properties for Port-Said West [9, 13].

2.5 Construction stages

The analysis is divided into four construction stages and described as follows:

- "Initial phase" directly generates initial effective stresses, pore pressures, and state parameters,
- "Construction" consolidation analysis of the model considering the construction of the tank in 1 [day],
- "Loading" consolidation analysis of the model which applies the loads on the cylindrical tank in 1 [day] and
- "Final Consolidation" consolidation analysis in which the model reaches minimum excess pore pressure equal to 1 [kN/m²].

2.6 Results and discussion

The circular tank described earlier in section 2.1 was analyzed numerically by El-Gendy [6] using ELPLA software with the multi-layer soil model. For the validation of the analysis features and techniques explained in the previous sections, this problem was re-analyzed here by PLAXIS 3D. Figure 2.3 compares the settlement results of both analyses along the tank diameter. The settlement results in the vicinity of the tank center (obtained herein by PLAXIS 3D) match well with those obtained by ELPLA, whereas a maximum difference of approximately 15% to the conservative side occurred at the tank corner.

The resulting settlement of the tank was unacceptable as it exceeded 41.5 [cm] all over the tank base, as shown

in Figure 3.2. Figure 3.3 shows the variation of final settlement at the tank center with time elapsed (in years) after finishing the construction. The consolidation reached 9.32 and 10.83 [cm] after 5 and 50 [years], respectively.

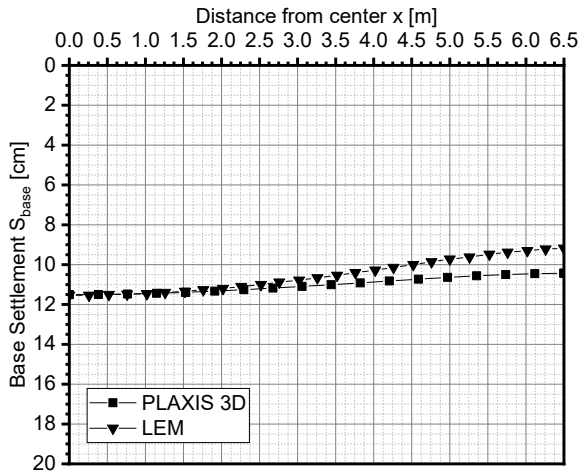


Figure 2.3: Comparison of base settlement of a circular tank located at Port-Said West.

3 NUMERICAL ANALYSIS AND DISCUSSIONS

A cylindrical fully-filled water tank resting on the ground at Port-Said West with an outer diameter of $d = 20$ [m] and a height of $H = 6$ [m], serves as a fundamental case study for the current research. As illustrated in Figure 3.1, the thickness of the wall was taken as $t_w = 0.3$ [m], whereas the base thickness $t_B = 0.5$ [m]. Material properties of the tank and the unit weight of water are provided in the figure. Soil modeling and characterization follow the description in the preceding section.

3.1 Stone columns

Stone columns were chosen as the first alternative to improve the soil's load-bearing capacity and mitigate the tank settlement. It's well understood that stone columns can distribute the loads on compressible soils more efficiently as they accelerate the consolidation process. For the present study case, a group of stone columns of the same diameter and height were distributed under the tank base according to the pattern shown in Figure 3.4. This completely symmetric group of stone columns consists of 49 columns aligned along three imaginary co-center circles of 6, 12, and 18 [m] diameter, respectively, in addition to a single column at the tank center. The study covers three different diameters of the stone column, $DSC = 1, 1.25, \text{ and } 1.5$ [m], whereas the column height was either 12.5, 25, 37.5, or 50 [m]. Under these conditions, the closest distance between any adjacent pair of stone columns ranges from 2 to 3 times the diameter of the stone column.

Moreover, the total replacement area covered by the stone columns reaches 12.25%, 19.14%, and 27.56% of the circular base area for the three different diameters

under consideration, respectively. Although the recommended ratio of replacement area for stone columns ranges from 10% to 20% according to previous studies [14, 15], this ratio was raised to 27.56% in some additional study cases herein to cover a broader range of design cases. The material properties of the stone column used in the present study were taken as given in Table 3-1, Yoo (2010) [16].

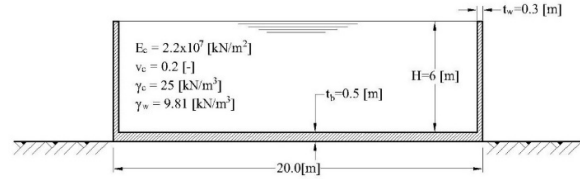


Figure 3.1: Study case of a circular water tank.

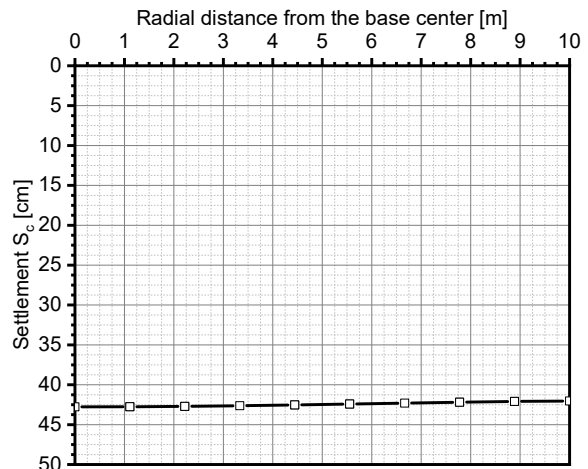


Figure 3.2: Anticipated final settlement of the tank base.

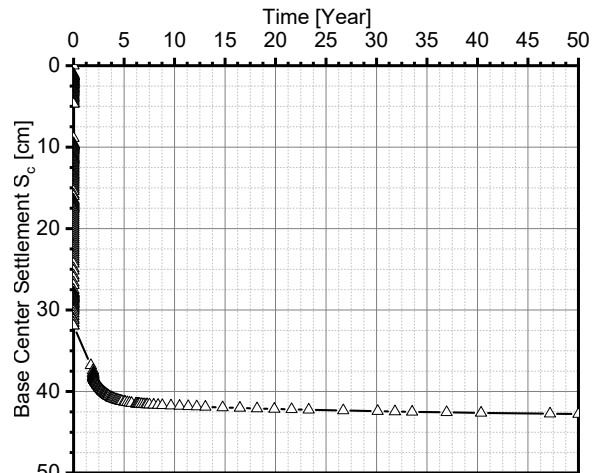


Figure 3.3: Final settlement at the center of the tank base.

Table 3-1. Material properties of stone columns (Mohr-Coulomb constitutive model)

Property	Value	Unit
Sat. unit weight	23	[kN/m ³]
Young's modulus	40,000	[kPa]
Poisson's ratio	0.3	[-]
Cohesion	5	[kPa]
Friction angle	40	[deg]
Dilation angle	10	[deg]
Initial void ratio, e_o	0.3	[-]
Permeability, k_v	1.2×10^{-4}	[m/s]

Figure 3.5 shows the total settlement under the center of the base plate (positive when downward) over 50 years for various values of diameter and height of the stone column. The results indicate that the soil resistance to deformation increased, resulting in decreased soil settlement with an increase in both stone column height and diameter.

The settlement at the center of the tank base for a stone column diameter D_{SC} of 1 [m] is smaller than the central settlement of the control case by 17.11%, 34.18%, 39.79%, and 42.79%, for column heights of 12.5, 25, 37.5, and 50 [m], respectively. For a stone column with $D_{SC} = 1.25$ [m], the center settlement decreases by 21.30%, 41.52%, 49.31%, and 55.16%, respectively. Additionally, for a stone column diameter of $D_{SC} = 1.5$ [m], the center settlement decreases by 22.45%, 42.27%, 54.87%, and 65.23%, respectively. The results reveal that the settlement reduction at the center of the tank base is more sensitive to variations in the stone column height than the stone column cross-sectional area. In other words, the increase in stone column height could control the settlement of the tank more efficiently than the increase in stone column area. These findings agree with previous studies [14, 15].

Figure 3.6 illustrates the consolidation curves over time at the center of the tank base for a diameter $D_{SC} = 1$ [m] and various heights of the stone columns. It is observed that for $H_{SC}=12.5$ [m], the initial settlement at the center of the tank base accounts for 78.73% of the total settlement. Over five years, the total settlement increases to 94.81% of the final settlement (or the settlement over 50 years). Similarly, for $H_{SC}=25$ [m], the initial settlement and the settlement after five years at the center were found to be 77.34% and 95.80%, respectively, relative to the settlement after 50 years. Those ratios were 77.14% and 96.74%, respectively, for $H_{SC}=37.5$ [m]; and 77.69% and 97.20%, respectively, for $H_{SC}=50$. The corresponding results for $D_{SC} = 1.25$ [m] and $D_{SC} = 1.5$ [m] are shown in Figure 3.7 and Figure 3.8, respectively. For $D_{SC} = 1.25$ [m], the initial settlement accounts for about 81% of the settlement after 50 years, while the total settlement over five years reaches 94.24% and 97.11% of the settlement after 50 years for $H_{SC}=12.5$ [m] and $H_{SC}=50$ [m], respectively. For $D_{SC} = 1.5$ [m], the initial settlement accounts for about 82% of the settlement after 50 years, while the total settlement over five years reaches 93.75% and 96.97% of the settlement after 50 years for $H_{SC}=12.5$ [m] and $H_{SC}=50$ [m], respectively.

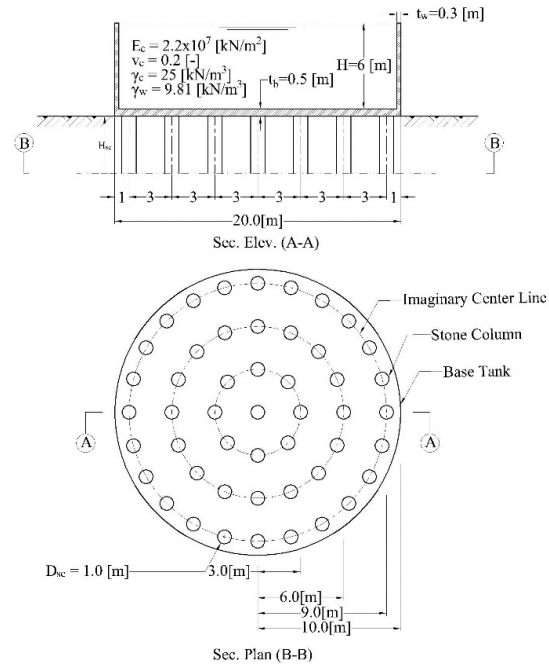


Figure 3.4: Stone column arrangement.

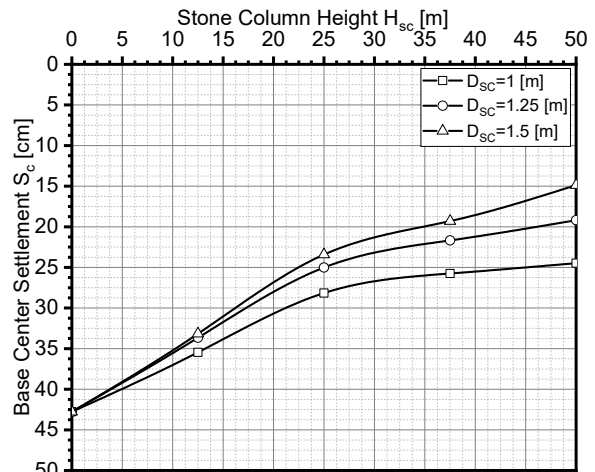


Figure 3.5: Variation of settlement with the height of the stone column at the center of the tank.

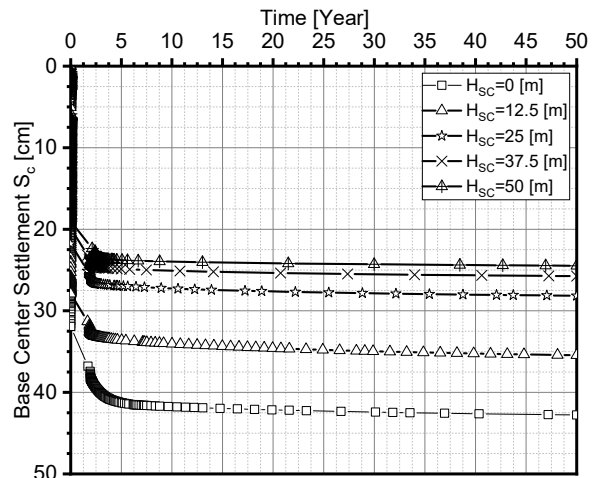


Figure 3.6: Time-settlement response at tank-center when the diameter of stone columns $D_{SC}=1$ [m].

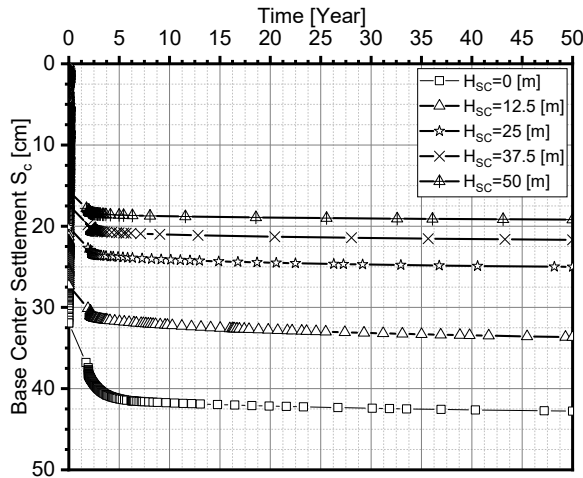


Figure 3.7: Time-settlement response at tank-center when the diameter of stone columns $D_{SC}=1.25$ [m].

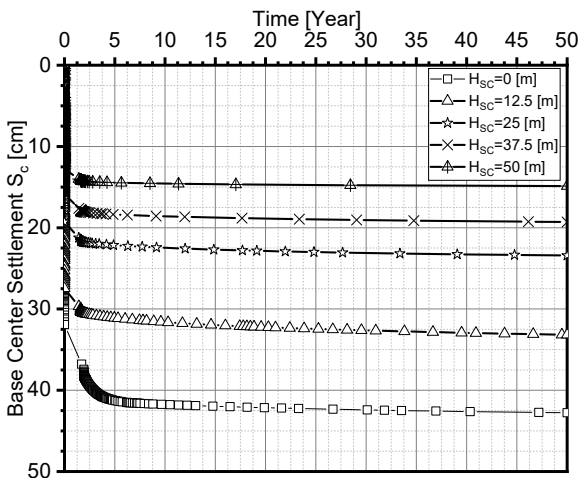


Figure 3.8: Time-settlement response at tank-center when the diameter of stone columns $D_{SC}=1.5$ [m].

3.2 Encased stone columns

Encased Stone Columns are a ground improvement technique in which individual stone columns are installed vertically into the ground at specified spacing. These columns are then encased in a sheath of geotextile or geogrid materials to provide confinement and to create a composite structure. They offer a cost-effective and efficient solution for mitigating settlement issues in challenging soil conditions. The completely symmetric group comprising 49 stone columns, shown in Figure 3.4, which was analyzed earlier, is reconsidered herein. Now, it is assumed that every column is encased in a sheath of geogrid. The diameter and height were kept constant for all columns in every study case. The study covers three different diameters and four different heights of the stone column ($D_{SC} = 1, 1.25, \text{ and } 1.5$ [m], and $H_{SC} = 12.5, 25, 37.5, \text{ and } 50$ [m]). The material properties of the stone column were taken as the previous section following Yoo (2010) [16] as given in Table 3-1. The encasement stiffness was taken as 2500 [kN/m].

Figure 3.9 shows the total settlement under the center of the base plate over 50 years for various values of diameter and height of the encased stone column. The results indicate that soil settlement decreases with an increase in either the height or the diameter of the encased stone columns. The settlement at the center of the tank base for a stone column of diameter $D_{SC} = 1$ m is smaller than the central settlement of the control case by 23.38%, 40.96%, 46.64%, and 50.27%, for column heights of 12.5, 25, 37.5, and 50 m, respectively. For a stone column with $D_{SC} = 1.25$ m, the center settlement decreases by 24.43%, 45.59%, 53.29%, and 59.86%, respectively. Finally, for $D_{SC} = 1.5$ m, the reductions in the center settlement were 25.02%, 47.56%, 57.10%, and 67.83%, respectively.

Increasing the diameter of relatively short columns (i.e., $H_{SC} = 12.5$ m) has a trivial effect (i.e., less than 2%) on the settlement. As the column height H_{SC} becomes higher, reductions in the final settlement resulting from a diameter increase become more pronounced. For instance, the percentage reduction in the settlement would be 17.56% more if the column diameter changed from 1 m to 1.5 m.

The consolidation curves over time at the center of the tank base for various diameters and heights of the encased stone columns are shown in Figure 3.10 to Figure 3.12. It is evident that the majority of settlement occurs initially in all cases. The initial settlement accounts for about 80% to 87% of the final settlement (or the settlement over 50 years). The ratio of initial to final settlement is lower for smaller diameters of stone columns. Moreover, for smaller diameters of stone columns (i.e., $D_{SC} = 1$ m), this ratio would be almost constant regardless of variations in the diameter or length of the encased stone column. Likewise, for $D_{SC} = 1$ m, the settlement over five years represents approximately 96% of the final settlement for all heights of stone columns under consideration. For larger diameters ($D_{SC} = 1.25$ and 1.5 m), the ratio of settlement over five years to the final settlement ranges from 93% to 97%.

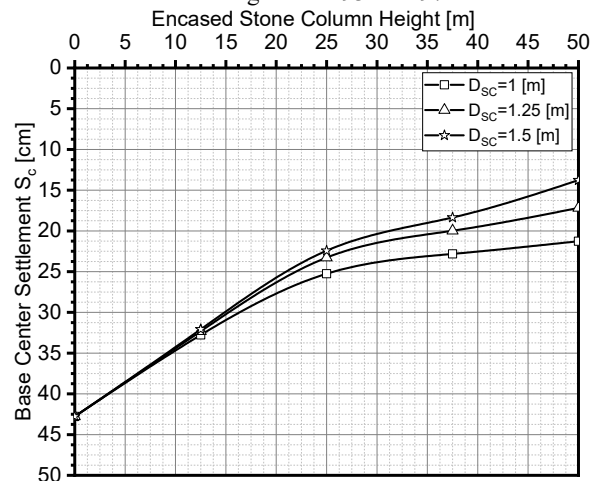


Figure 3.9: Variation of settlement with the height of the encased stone column at the center of the tank.

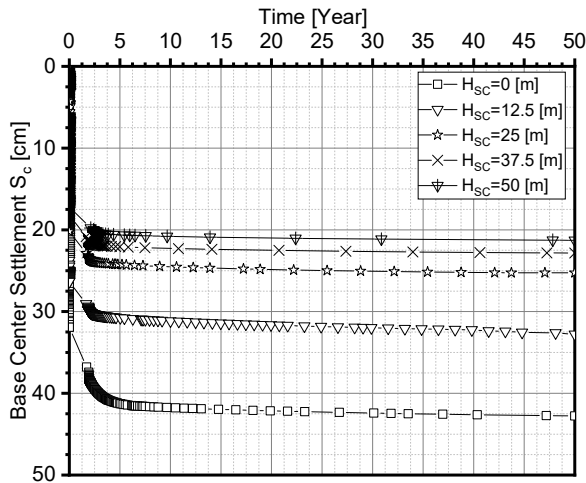


Figure 3.10: Time-settlement response at tank-center when the diameter of encased stone columns $D_{sc}=1$ [m].

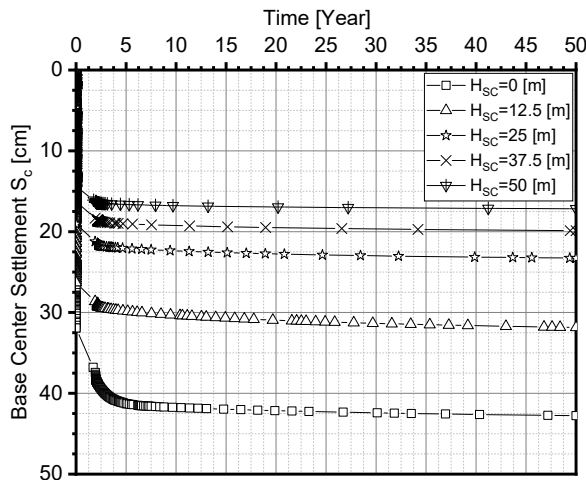


Figure 3.11: Time-settlement response at tank-center when the diameter of encased stone columns $D_{sc}=1.25$ [m].

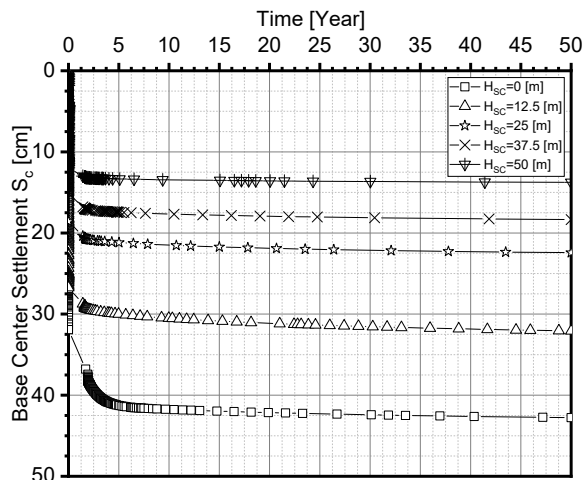


Figure 3.12: Time-settlement response at tank-center when the diameter of encased stone columns $D_{sc}=1.5$ [m]. Lowering the foundation level of the tank.

3.3 Lowering the foundation level of the tank

Lowering the foundation level helps to reach more stable soil layers and effectively reduces the anticipated settlement of the tank, especially if the original intent was to erect the tank directly on the more compressible soil strata at the ground surface. Figure 3.13 presents the total settlement at the center of the tank base for different values of the foundation level with reference to the natural ground surface as the zero level. It can be observed that the settlement at the tank base improves noticeably as the foundation level becomes lower. In the study case under consideration, about one-half of the anticipated final settlement at the tank center could be avoided by erecting the lower third of the tank height under the ground surface. If one-third of the tank height were erected under the ground surface, more than 60% of the anticipated final settlement at the tank center could be excluded. Finally, about two-thirds of the final settlement at the tank center could be avoided by erecting two-thirds of the tank height below the ground surface.

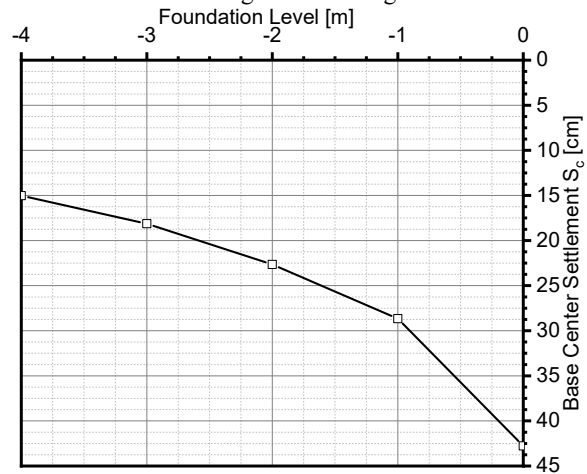


Figure 3.13: Variation of center settlements in the base plate (positive when downward) for difference tank footing level.

3.4 Comparison of results

This section compares the efficiency of three settlement mitigation techniques examined in this study. The selection of these techniques is based on their common use in practice, namely, stone columns, encased stone columns, and variation in foundation level. The settlement-time responses over a 20-year period at the center of the circular base are compared in Table 3-2 and Figure 3.14 for the three different techniques. The results for both stone column improvement techniques, with and without encasement, are presented for a 1.5m diameter and 50m height stone column, with the tank base resting on the ground surface. Meanwhile, the results for the third alternative are provided for the case where the foundation level of the tank base is 4m below the ground surface.

In the study cases involving stone columns, with or without encasement, the settlement-time response at the tank center appears to be similar for both soil improvement techniques. However, the resulting

settlement would be slightly larger in the absence of encasement due to the lower stiffness of the stone column in such cases. The majority of settlement occurs initially, and the consolidation rate is pronounced during the first couple of years, diminishing drastically thereafter, with only approximately 3% of the final settlement occurring over the next 18 years.

In contrast, for the third alternative, where the foundation level of the tank was lowered, the settlement-time response appears markedly different. The initial settlement is relatively smaller as the share of settlement in the top 4m of the natural soil is eliminated in this case. The consolidation of the natural soil layers continues over much longer time periods until the final settlement occurs.

Table 3-2. Settlement values in time for alternative methods

Settlement mitigation technique	Settlement (in centimetres) over various time periods (in years)							
	S_i	S_{1y}	S_{2y}	S_{3y}	S_{4y}	S_{5y}	S_{10y}	S_{20y}
Control model	31.94	36.17	38.40	40.10	40.90	41.26	41.75	42.14
Stone columns	12.76	13.88	14.29	14.37	14.42	14.44	14.56	14.70
Encased stone columns	11.97	12.90	13.19	13.25	13.30	13.34	13.48	13.58
Foundation level is 4m lower	9.75	10.52	10.85	10.94	10.99	11.05	11.96	13.01

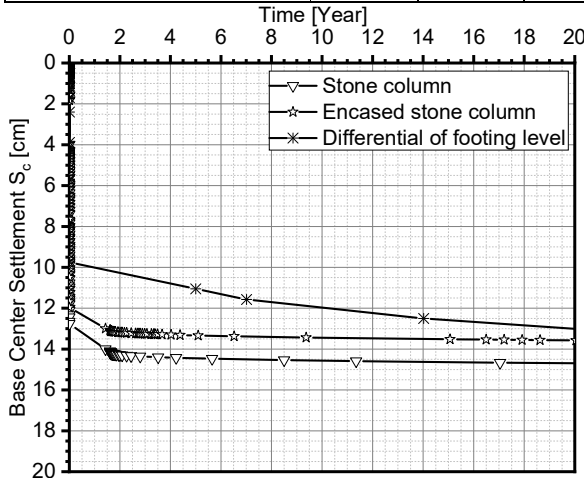


Figure 3.14: Settlement response at the tank center for three different mitigation techniques.

4 CONCLUSIONS

This study discussed three alternatives to mitigate the anticipated excessive settlement of the cylindrical tanks full of water on Port-Said West's weak soil. These alternatives include soil improvement by using either the stone columns or encased stone columns and lowering the foundation level of the tank with no soil improvement. A prime research objective was to evaluate the efficiency of those alternatives in mitigating the settlement of circular storage tanks constructed at Port Said. A 3D nonlinear finite analysis was undertaken for layered soil represented by the Mohr-Coulomb and Hardening constitutive models. From the present study, the following conclusions could be drawn:

- 1 The settlement of the cylindrical tanks decreases with the increase in the height or diameter of stone columns, whether provided with a geogrid encasement. The larger the diameter and the greater the height of the stone columns, the lower the anticipated settlement of a circular tank constructed at Port-Said West.

- 2 Encased stone columns are slightly more efficient than stone columns in mitigating settlement. The majority of the anticipated settlement for both techniques occurs within the first two years, with no more than 3% of the final settlement occurring over the next 18 years of the tank's lifespan.
- 3 For short encased stone columns (i.e., Stone column height = 12.5m), the anticipated settlement of a circular tank constructed in Port-Said West is not sensitive to variations in the diameter of stone columns.
- 4 For the study case under consideration, approximately half of the anticipated final settlement at the tank center could be avoided by erecting the lower third of the tank height below the ground surface. If half of the tank height were erected below the ground surface, more than 60% of the anticipated final settlement at the tank center could be excluded.
- 5 The three alternatives of settlement mitigation discussed in this study could eventually achieve accepted results with respect to the anticipated settlement of the tank. From an economical perspective, lowering the tank foundation level is the most cost-effective option, as it doesn't need any additional resources. In this case, the final settlement occurs over a longer time period if compared to the stone column improvement techniques.

5 REFERENCES

- 1 Wang, G., "Consolidation of Soft Clay Foundations Reinforced by Stone Columns under Time-Dependent Loadings," *Journal of Geotechnical and Geoenvironmental Engineering*, vol. 135, no. 12, pp. 1922-1931, 2009.
- 2 Deb, K., & Das, A. K., "Distribution of Stress on Stone Column-Reinforced Soft Soil under Cylindrical

- Storage Tank," *Applied Mechanics and Materials*, vol. 567, pp. 699-704, 2014.
- 3 Das, A. K., & Deb, K., "Response of Cylindrical Storage Tank Foundation Resting on Tensionless Stone Column-Improved Soil," *International Journal of Geomechanics*, vol. 17, no. 1, 2017.
 - 4 Zukri, A., & Nazir, R., "Numerical modelling techniques of soft soil improvement via stone columns: A brief review," *IOP Conference Series: Materials Science and Engineering*, vol. 342, 2018.
 - 5 Muzammil, S. P., Varghese, R. M., & Joseph, J., "Numerical Simulation of the Response of Geosynthetic Encased Stone Columns Under Oil Storage Tank," *International Journal of Geosynthetics and Ground Engineering*, vol. 4, no. 1, 2018.
 - 6 El-Gendy, O., Behavior of Tanks under Static and Cyclic Loading, Port Said: Port Said University, 2016.
 - 7 Killeen, M. M., & McCabe, B. A., "Settlement performance of pad footings on soft clay supported by stone columns: A numerical study," *Soils and Foundations*, vol. 54, no. 4, pp. 760-776, 2014.
 - 8 El-Gendy, M. and El-Gendy, A., "Analysis and Design of Slab Foundations by FE-Method- Program ELPLA 10," GEOTEC Software Inc., Canada, 2015.
 - 9 Pelli, F. and Rossanese, A. (2000), "Settlements of an Instrumented Landfill on Soft-Delta Soil with Vertical Wick Drains," in *International Conference on Geotechnical & Geological Engineering*, Melbourne, Australia, November 2000.
 - 10 Banupriya S, Soundarya M.K, and P.R. Kalyan Chakravarthy, "Stress-Strain and Strength Characteristics of Sand-Silt Mixtures," *International Journal of Latest Trends in Engineering and Technology (IJLTET)*, vol. 6, no. 1, September 2015.
 - 11 Al-Khafaji, A., Maillacheruvu, K., Jacobs, R., Pellicer, E., Adam, J. M., Yepes, V., Singh, A., & Yazdani, S. , "Analysis of Empirical Compression Index Equations Using the Void Ratio," *Proceedings of International Structural Engineering and Construction*, vol. 4, no. 1, 2017.
 - 12 Terzaghi, K., Peck, R.B. and Mesri, G., Soil Mechanics in Engineering Practice, New York: John Wiley and Sons, Inc., 1996.
 - 13 Pelli, F. and Carletti, A., "Characterization of soft deposits in the Eastern Nile Delta," in *Proceedings 1st Int. Conf. on Site Characterization ISC'98*, Atlanta, USA, 1998.
 - 14 Barksdale, R. D. and Bachus, R. C., "Design and construction of stone columns," Office of Engineering and Highway Operations Research and Development, Federal Highway Administration, Washington, D.C., 1983.
 - 15 Raithel, M., Kempfert, H. G., and Kirchner, A., "Geotextile-encased columns (GEC) for foundation of a dike on very soft soils," in *Proc., 7th Int. Conf. on Geosynthetics*, Balkema, The Netherlands, 2002.
 - 16 Yoo, C., "Performance of Geosynthetic-Encased Stone Columns in Embankment Construction: Numerical Investigation," *Journal of Geotechnical and Geoenvironmental Engineering*, vol. 136, no. 8, pp. 1148-1160, 2010.